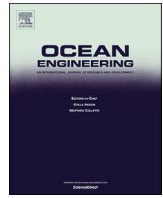University of
Strathclyde
Glasgow

Reich, Andrew and Payne, Grégory S. and Pascal, Remy and Spinneken, Johannes (2018) Investigation into wave basin calibration based on a focused wave approach. Ocean Engineering, 152. pp. 181-190. ISSN 0029-8018 , http://dx.doi.org/10.1016/j.oceaneng.2018.01.044

This version is available at https://strathprints.strath.ac.uk/62828/

Investigation into wave basin calibration based on a focused wave approach

Andrew Reich [a], Grégory S. Payne [b,*], Remy C.R. Pascal [c], Johannes Spinneken [d]

[a] 400 Ridley Street, Corydon, IN 47112, US
[b] Department of Naval Architecture, Ocean & Marine Engineering, University of Strathclyde, Henry Dyer Building, 100 Montrose Street, Glasgow G4 0LZ, UK
[c] INNOSEA, ETTC, Alrick Building, Max Born Crescent, Edinburgh EH9 3BF, UK
[d] Evergreen Innovations Ltd., 79 Tonbridge Road, Tonbridge TN11 9BH, UK

ABSTRACT

The purpose of this paper is to present a detailed numerical investigation concerning the calibration of force controlled wave generation facilities. The methodology is presented for a 2-dimensional calibration; the findings being equally applicable to the calibration of 3-dimensional wave basins. State-of-the-art force controlled wavemaking facilities comprise sophisticated hardware, software and control systems, commonly incorporating active absorption mechanisms. Such facilities have the potential to reproduce ocean wave of exceptional quality, but poor understanding of accurate calibration processes often hinders full exploitation. A technique based upon the generation of focused wave events may offer a very accurate and time-efficient calibration. However, such a methodology may lead to erroneous results if not employed correctly. The theoretical and statistical analysis presented herein investigates the sensitivity of such method to a number of important parameters. The results obtained are directly applicable to a large number of hydrodynamic facilities.

1. Introduction

Tank testing is a key research and development tool in many fields of marine engineering. These include naval architecture, coastal engineering, the offshore oil and gas industry and more recently the marine renewable energy sector. Experimental work in these fields comprises, but is not limited to, wave breaking, extreme wave loadings and large amplitude motions of floating bodies. The complexity of these physical phenomena often means that their theoretical or numerical modelling is still challenging and experimental data are therefore required for design purposes or for validating the models. Tank testing makes it possible to obtain these experimental results in an accessible and controlled environment at only a fraction of the cost of sea trials.

An important aspect of tank testing is the control of the wave generation process. A large proportion of wave tank testing facilities are equipped with force controlled wavemakers of the type developed by the company Edinburgh Designs (www.edesign.co.uk). More than 85 wave basins across 23 countries are indeed fitted with Edinburgh Designs wave making apparatus which amount to over 1 500 wave paddles worldwide. The force control feature of this wave making technology allows active wave absorption and the generation of spectra of waves with a high degree of fidelity but it also means that the apparatus must be considered as a hydrodynamic feedback system. As a dynamic electromechanical

device, the generation system will react differently to each input frequency. If left uncorrected the dynamic phenomena will result in unexpected wave generation that does not match the desired input from the user. However by identifying and subsequently correcting for the tank's dynamics, accurate and repeatable recreation of the desired sea state can be achieved. Such a tank is said to be calibrated, thus the process of identifying the proper correction factors is known as calibration. Because the underlying dynamics of each tank are a function of the entire system, the response of a particular tank is unique and requires a unique set of correction factors.

To some extent, the operation of force controlled wave machines can be derived theoretically. Spinneken and Swan (2009a) derived a theoretical relationship (also referred to as 'transfer function') between the input signal to the wave generation system and the resulting wave generated for wavemakers controlled in force-feedback, accounting for second order wave effects. The validity of their theoretical analysis was investigated in Spinneken and Swan (2009b), and an extension of their theory appropriate to the operation of 3D wave basins is presented in Spinneken and Swan (2012). In the context of these theoretical formulations, second-order wave effects include both second-order wave-wave interactions and second-order wave-structure interactions due to the presence of the wavemaker. These interaction models are developed as perturbation expansions of the potential flow governing equations,

which are then truncated at the second-order of the expansion parameter (usually the wave steepness), and subsequently solved analytically. Even without taking into effect realistic wave tank effects such as transfer function discontinuities, this leads to very challenging analytical problems. To date, there is no consistent framework that addresses both second-order wavemaker effects and realistic tank effects.

A theoretical calibration function is a good starting point but it is often useful to refine it experimentally given that the theoretical models do not generally account for every single aspect of the complex electromechanical process of wave generation. The most common way to calibrate wave tanks is based on regular waves. In this method, one regular wave is produced in the tank at a time, and the tank output is compared with the desired user input to determine the appropriate correction factor. The process is then repeated for a range of frequencies. The regular wave method is highly accurate and generally easy to perform, but can be time-consuming to implement fully as the calibration is carried out for only one frequency component at a time. Compounding the problem, three or more iterations of the process may be necessary to determine the correction factors with a high degree of accuracy. In a three-dimensional wave basin the calibration must be performed separately over a range of directions.

A less time-consuming alternative to the regular wave approach is to generate a spectrum of waves at the desired calibration frequencies concurrently in the tank. The resulting sea state can then be compared with the desired spectrum, and correction factors for each frequency can be calculated simultaneously. Such a broadband approach reduces the total number of required runs significantly but can be affected by wave reflection. Sufficient time must pass to allow the generated waves to propagate to the measurement location. The amount of time required is dependent on the highest frequency component (which has the slowest velocity). At the same time, waves reflected from the edges of the tank will begin to interfere with measurement after a certain period. The time reflected waves take to return to the measurement location is dependent on the lowest frequency component (which has the fastest velocity). Thus the uncorrupted time period for a broadband approach is significantly shorter than that of the regular wave technique.

In an attempt to overcome the problems associated with wave propagation and reflection, Masterton and Swan (2008) proposed the use of a focused spectrum. In their approach, the component waves are 'focused' through phase modification so that they come into phase at the measurement location during the uncorrupted time period. This technique concentrates the wave energy around the focal point, ensuring that wave energy outside the uncorrupted region is minimal. The original purpose of the method described by Masterton and Swan (2008) was to calibrate the wave tank to accurately reproduce a particular type of focused event desired by the authors, and it was shown to be very effective at achieving this goal.

The present study was motivated by numerically investigating the use of this method to calibrate force controlled wavemakers for accurate reproduction of more generic sea states. This investigation highlighted cases where the technique may lead to erroneous results. This could happen for wet back wavemakers or when the wave tank has previously only been calibrated for a subset of its wave generation spectrum. Section 2 summarises the existing calibration methods, and further highlights the need for such procedures. Section 3 illustrates the potential pitfalls of the method with a clear example. The underlying reasons for those pitfalls are then described (section 3.2) and mitigations approaches are explored (section 3.3). Section 4 provides an in depth statistical analysis of numerical simulations designed to assess the calibration method's performance. To that end, formalised calibration metrics are first devised to quantitatively assess the success of the calibration procedure. Finally, section 5 concludes the present work and makes recommendations for improved wave tank calibrations.

In all the numerical simulations used in this study, wave propagation is modeled using linear theory. As a result, the findings may not be directly applicable to the generation of large focused wave groups or

steep random sea states. However, steep wave group generation may still benefit from the methodologies outlined. Assuming an appropriately large distance between the wave group focus location and the wavemaker, the wave group is relatively dispersed at the wavemaker, where local nonlinearity is hence limited. The approach introduced here is likely to remain beneficial. For steep random sea states, nonlinearities will inevitably occur at the wavemaker location, and generation based upon second-order random wavemaker theory may be more suitable than an empirical calibration. While it is difficult to define an exact upper limit of linear theory in random sea states, a value of $\frac{1}{2} \cdot H_s \cdot k_p = 0.02$ (product of significant wave height H_s and wave number corresponding to peak period, k_p) can be taken as an approximate limit for linear theory to remain valid (Latheef and Swan, 2013). In terms of focused wave groups, the limit of validity depends on both the steepness of the event to be generated and the location at which the event is to be reproduced (distance from the wavemaker). Linear theory is generally applicable if $A \cdot k_p \leqslant 0.05$ (product of maximum event amplitude A and peak wave number k_p). Nevertheless, with a sufficient distance from the wavemaker, even large overturning or breaking wave groups may be dispersed and near-linear at the wavemaker.

2. Wave tank calibration

2.1. Definition of a tank transfer function

At this stage the concept of a tank calibration and a tank transfer function should be further clarified. For non-absorbing position-controlled wave machines a transfer function is simply represented by the well known wave-amplitude ratio, and extensive reference to this can be found in Havelock (1929), Biésel and Suquet (1954) and Ursell et al. (1960). It has long been established that a wavemaker produces both evanescent and progressive wave modes. The evanescent wave modes arise as a local effect in the proximity of the wavemaker, decay quickly with increasing distance from the wavemaker. In contrast, the progressive wave mode propagates into the wave flume or wave basin, and the model in the testing area is consequently only subjected to these latter modes.

The transfer function in position control solely addresses the relationship between the wave board displacement and the progressive wave. In a more general wave-body interaction context, the progressive wave may be regarded as the radiation damping, and this damping term must be in phase with the oscillator's velocity. In other words, the displacement of the wave board and the surface elevation due to the progressive wave (evaluated on the wave board) are 90° out of phase; this phase shift being frequency independent. In summary, the transfer function in position control is characterised by the wave-amplitude ratio and a 90° phase shift between the wave-board displacement and the progressive wave mode.

Considering the transfer function appropriate to force-controlled wave machines (as those developed by Edinburgh Designs), this incorporates the absorption mechanism, and directly relates to the hydrodynamic forces acting on the machine. In contrast to position control, the resulting transfer function is characterised by an amplitude *and* a phase relation. A detailed analysis of such a transfer function is outside the scope of the present work, and the reader is directed to Spinneken and Swan (2011, 2012). In the context of the present work, a 2-dimensional theoretical transfer function Spinneken and Swan (2011) will be used as a reference case within the analysis presented in sections 3 and 4.

2.2. The purposes of wave tank calibration

The exact purpose of a wave tank calibration somewhat depends on the user's testing strategy and environment. The focused wave tank calibration discussed herein may be used
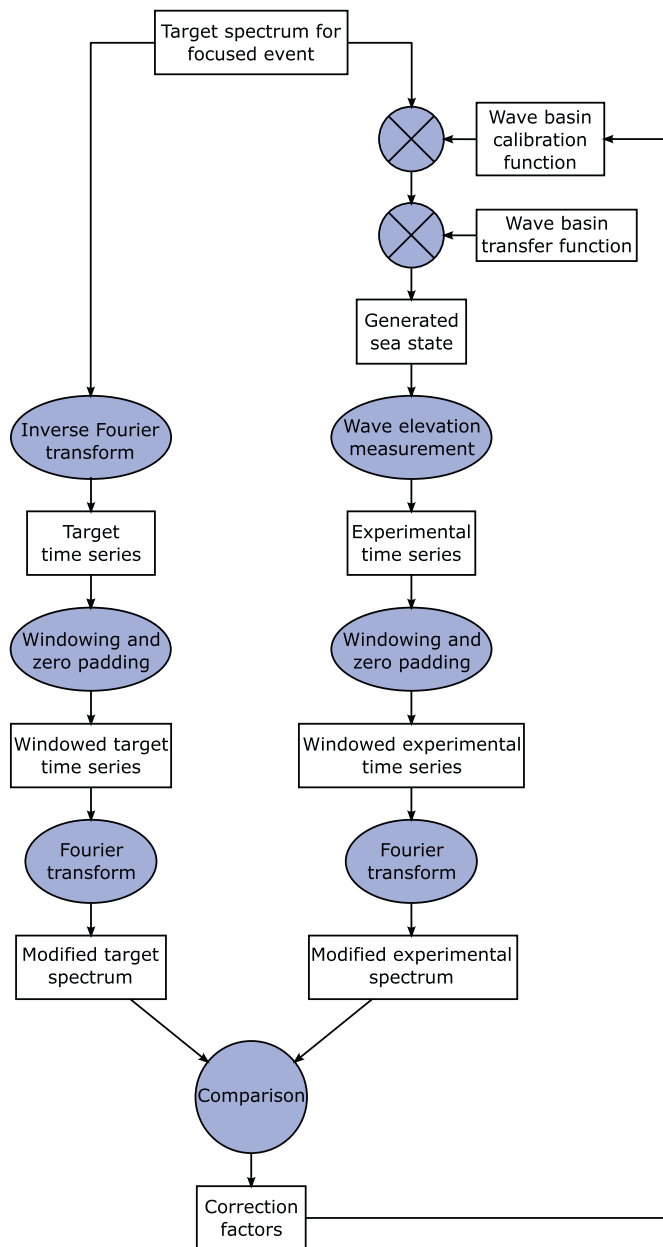
Fig. 1. Iterative focused event calibration process.

1. to subsequently create focused wave events, and these may be unidirectional or directionally spread. This is commonly undertaken in the investigation of large amplitude wave-structure loading or to underpin the understanding of wave-wave interactions.
2. to obtain a broad banded calibration of the wave tank, and to subsequently adopt this calibration in creating random wave spectra with a specified amplitude or energy content. In this context, the phase calibration is of secondary concern, as the wave phases are fully randomised during the experimental investigation.
3. to obtain a particular time series of water surface elevation at predetermined points in the tank. In this latter case the phase information is of paramount importance, as it determines the overall alignment of individual wave components.

Consequently, any accurate calibration procedure must improve the performance of the three above criteria. This requires an assessment of (a) the quality of focused events, (b) the quality of random phase spectra and (c) the quality of time series reproductions. Performance measures

for (a) - (c) will be introduced in §4.1.

2.3. Focused wave calibration technique

Given that the present study relies partly on the focused wave calibration method developed by Masterton and Swan (2008), it is thought useful at this stage to provide a brief summary of the technique. More detail can be found in Masterton and Swan (2008). The method applies to facilities using deterministic wave generation, for which the command signal to the wave makers is derived through an inverse Fourier transform of a target spectrum. This means that the sea states generated are periodic and that their period (or repeat time) is equal to $1/\Delta f$, where Δf is the frequency resolution of the target spectrum.

The calibration process is as follows:

1. A target spectrum is first chosen and the phase of each frequency component is adjusted to generate a focused wave.
2. The wave elevation is experimentally measured in the basin. The measurements are not taken over the full repeat time of the sea state but only over a short time window centred on the focused wave event. This avoids the measurements to be corrupted by wave reflection. The focusing of the wave means that most of the spectrum's energy is contained within the short time window.
3. The resulting time series is 'extended' by zero padding so that its overall duration is equal to the full repeat time of the original sea state. This means that after a Fourier transform, the resulting spectrum, called 'modified measured spectrum', has the same frequency resolution as the target spectrum.
4. The target spectrum is turned into a virtual target wave elevation time series through an inverse Fourier transform. The resulting time series is subjected to the same windowing and zero padding as the experimentally measured time series. It is then transposed back into the frequency domain through a Fourier transform to yield the 'modified target spectrum'.
5. The modified experimental spectrum is then compared to the modified target spectrum. From the discrepancies between both spectra, amplitude and phase correction factors are computed for each frequency component. These factors make up the wave tank calibration function.
6. A new experimental wave elevation time series is generated using the new calibration function. The new modified experimental spectrum is compared with the previously computed modified target spectrum.
7. The process is repeated from stage 2 and excluding stage 4, as the modified target spectrum only needs to be computed once. The iterative procedure is stopped when the modified experimental spectrum has converged towards the modified target spectrum; the entire process being illustrated by the schematic of Fig. 1.

3. Limitations of the methods and mitigation approaches

3.1. Potential pitfalls

The method developed by Masterton and Swan (2008) presents clear advantages when compared to the conventional regular wave calibration technique. It drastically reduces the number of wave measurement runs required and it greatly simplifies the handling of wave reflection. The method however comes with some pitfalls which, if not properly understood and carefully avoided, can lead to erroneous calibration functions despite the method apparently converging.

The main cause of these pitfalls lies in the zero padding process through which the values of a large portion of the wave elevation time series are assumed to be small. They are therefore not measured but simply set to zero. This makes the method performance very sensitive to discontinuities in the wave basin transfer function and in the initial calibration function used. The underlying theory of this process will be investigated in detail in section 3.2. At this stage, the potential
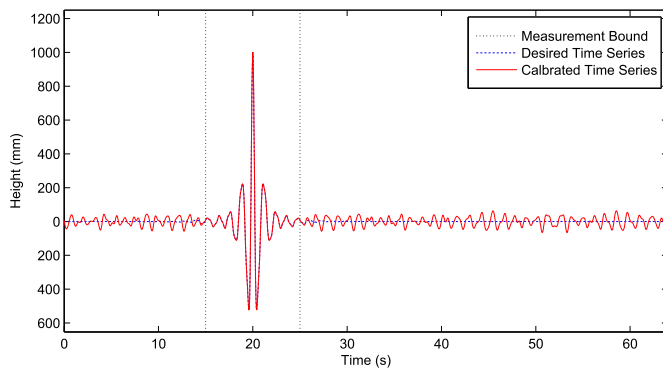
Fig. 2. Water surface elevation time series for the target spectrum and for the converged (calibrated) simulated spectrum.
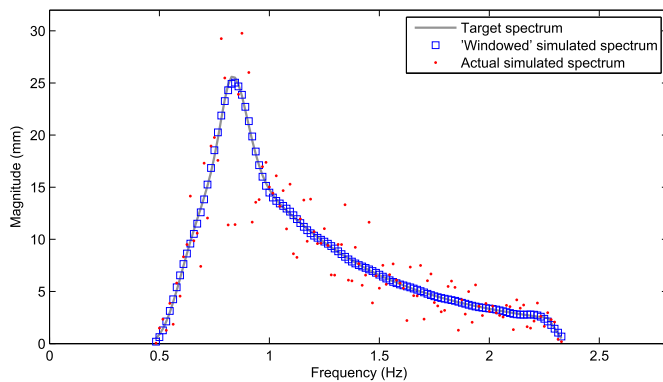

Fig. 3. Comparison of the water surface elevation spectra after calibration, including the spectrum associated with the simulated time series zero-padded outside the measurement window ('Windowed' simulated spectrum), the spectrum computed from the full time series (Actual simulated spectrum) and the target spectrum.
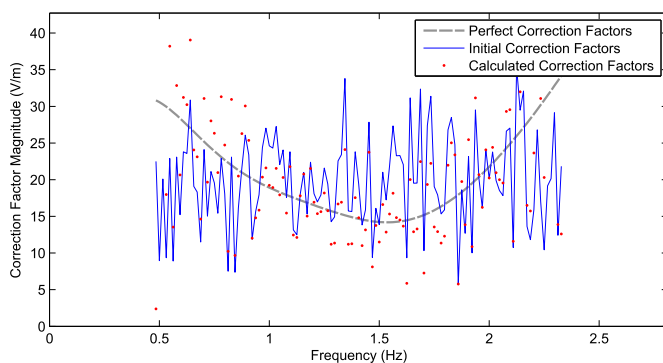

Fig. 4. Magnitude correction factors for the perfect, initial and computed calibrations.

limitations of the method are illustrated by an example derived through numerical simulation based on linear wave theory.

For the sake of simplicity, only one wave direction of propagation is considered. A virtual calibration is carried out for frequencies between 0.5 and 2.5 Hz using a focused JONSWAP spectrum with a repeat time of 64 s. The water surface elevation is recorded over a 20 s time window centred on the focused event.

Fig. 2 compares the target wave elevation time series (blue dashed line) with the one obtained after calibration (red solid line). It can be seen that within the measurement window, the match is excellent, hence the

successful convergence of the method. However when considering the intervals outside the measurement window and over the full repeat time of the spectrum, significant discrepancies can be observed.

Similar observations can be made in the frequency domain as illustrated in Fig. 3, where the target spectrum (grey solid line), the spectrum computed from the complete simulated time series after calibration (red dots) and the spectrum derived from the windowed simulated time series after calibration (blue squares) are considered. The latter time series is zero padded outside the measurement windows as explained in step 3 of section 2.3 and although the associated spectrum matches very well the target spectrum, the actual simulated spectrum (as derived from the full simulated time series and hence without zero-padding) exhibits significant discrepancies with the target spectrum. In fact, this observation was the main motivation for undertaking the work presented herein.

Fig. 4 compares the perfect calibration curve (grey dashed line), which corresponds to the inverse of the tank transfer function (Spinneken and Swan, 2011), with the correction factors obtained through the calibration method. It also shows the initial calibration curve (blue solid line) which was deliberately chosen to be highly discontinuous. It can be seen that the calculated correction factors poorly match the perfect calibration curve.

This example shows that for a strongly discontinuous initial calibration, the method can lead to erroneous correction factors. Moreover from a user point of view, the method can be deceptive. It does converge in that the generated spectrum computed from the windowed time series closely matches the target spectrum. However in a real tank of finite length, because of wave reflection, the user does not have easily access to the uncorrupted wave elevation time series over the full repeat time of the spectrum and hence cannot easily derive the true generated spectrum. The user has therefore no easy way to realise that the calibration achieved by the method is erroneous.

3.2. The impact of zero padding

As discussed above, the focused wave calibration method retains only a small portion of the full measured time series. Using this information alone would result in lower frequency resolution, making calculation of the correction factors more difficult. To overcome this problem, zeros are added to the time series, which gives the appearance of improved frequency resolution. However it is important to note that no new information is added by performing this operation. Instead, using Fourier analysis, it can be shown that this technique results in ideal sinc interpolation of the lower-resolution spectrum.

The net effect of this procedure is that a low-pass filter is applied to the true frequency spectrum (which is challenging to measure directly in short tanks due to wave reflection). Though the domains are reversed, the principle remains the same. In the case of the focused wave calibration method, the effect of the low-pass filter is dependent on the duration of the time window selected, and a shorter measurement duration results in more pronounced filtering.

Low-pass filtering of the frequency spectrum can lead to poor calibration performance. Correction factors are calculated by comparing the measured frequency spectrum with the target frequency spectrum, both of which have been low-pass filtered by means of post processing; effectively resulting in smoothed representations of the actual spectra. Therefore, the calculated correction factors will also necessarily be smooth. Smooth correction factors are not able to correct a non-smooth initial calibration function, nor are they able to converge to an non-smooth final calibration function, as may be needed to correct a non-smooth transfer function. As a result, it is important that both the initial calibration function and the transfer function be smooth enough to be unaffected by the low-pass filtering effect, or the calibration process may fail.

One way to eliminate the effects of low-pass filtering is to produce in the tank only the frequency components that can be discerned with the lower frequency resolution (which depend on the measurement
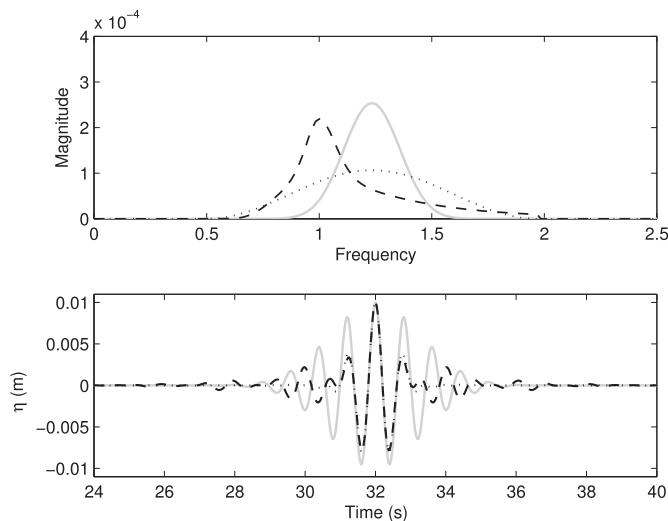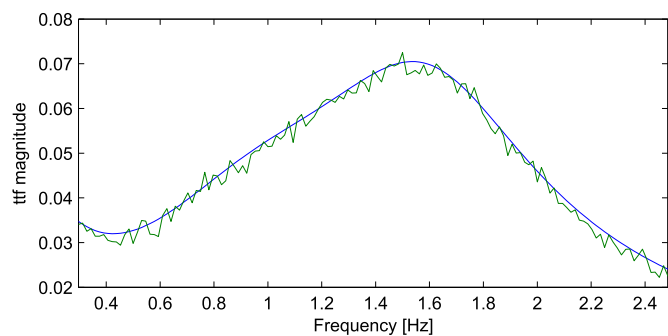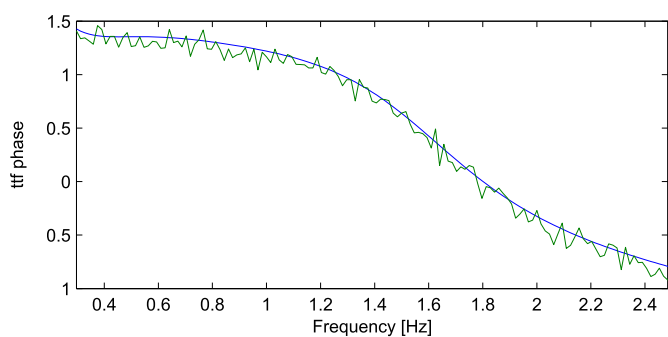
Fig. 5. Comparison of the frequency and the time domain representation of focused wave events based upon: ▬ ▬ JONSWAP spectrum, ⋯⋯ Hanning energy distribution and ▬▬ DPSS energy distribution.

(a) noise level introduced in tank transfer function magnitude

(b) noise level introduced in tank transfer function phase

Fig. 6. Representation of the tank transfer function (ttf) used within the numerical investigation. The non-smooth lines correspond to the highest level of noise introduced.

Table 1
Comparison of the energy contained within a certain time interval around the focused time.

Wave spectrum/Time interval	± 8s	± 4s	±2s
Top-hat	99.20%	98.34%	96.67%
Hanning	100%	99.99%	99.99%
Hamming	99.98%	99.97%	99.96%
Jonswap	99.99%	99.49%	95.20%
DPSS	100%	100%	100%

duration). These frequency components can then be calibrated directly without the need for zero padding. A disadvantage to this approach is that the frequency resolution of the calibration may be significantly lower than desired, especially in short tanks. However, interpolation can still be performed after the calibration has converged to populate the missing frequency components. Though interpolation will lead to some error, it eliminates the possibility of an erroneous calibration and relaxes the smoothness constraints on the initial calibration function and the transfer function.

3.3. Impact of the spectrum selection

The study by Masterton and Swan (2008) relied on a JONSWAP spectrum for calibration; this spectral shape being adopted to subsequently reproduce JONSWAP focused wave events in the wave basin. Experimental data suggests that this method is in fact very effective at accomplishing the goal of creating a JONSWAP focused event inside the measurement window (Masterton and Swan, 2008; Reich, 2010). However, it has also been demonstrated, that this method is not necessarily effective for a general calibration (Reich, 2010).

To apply zero padding as discussed above requires the surface profile to be close to zero in proximity of the focal time. In zero padding their data, Masterton and Swan (2008) chose a time interval of 8s around the focal time (±4s around 32s). Using a similar time and length scale to that considered in Masterton and Swan (2008), Fig. 5 illustrates both the frequency domain and the time domain representation of focused wave events based on a number of energy distributions. The wave phases have been aligned so that the energy focuses at $t = 32$s, and the maximum crest elevation is set to $\eta_{max} = 0.01$m.

The energy distributions considered in Fig. 5 are the Hanning distribution, the Digital Prolate Spheroidal Sequence (DPSS), and a typical JONSWAP spectrum. Both the Hanning and the DPSS distributions are centred around the mean frequency (1.25Hz) while a peak frequency of 1Hz has been chosen for the JONSWAP spectrum. The steepness values $A \cdot k_p$ associated with these focus events (as defined in section 1) are 0.04, 0.06 and 0.06 for the JONSWAP, Hanning and DPSS spectra respectively. The Hanning and DPSS spectra leads to mild non-linear conditions ($0.05 < A \cdot k_p \leqslant 0.1$) but the JONSWAP spectrum (used throughout this article) is within the linear limit ($A \cdot k_p \leqslant 0.05$). It is clear from Fig. 5 that the various energy distributions lead to very different focused events in the time domain. Most importantly, the energy contained within a certain time interval around the focused time may differ significantly.

This is further highlighted in Table 1, where a number of energy distributions are compared. In each case, the amount of energy within a particular time frame is normalised over the total energy contained in the spectrum. The data in Table 1 clearly confirms that the energy contained in a certain time interval depends on the energy distribution selected. While a time interval of 30s … 34s (±2s) accounts for 99.99% of all energy contained in a focused Hanning spectrum, this same interval would neglect approximately 4.8% of the energy contained in a focused JONSWAP spectrum. As a result, an energy distribution such as Hanning or Hamming may be more appropriate for a general purpose calibration. Care must be taken with the DPSS distribution, as this leads to a very narrow banded spectrum. This leads to the frequency components located toward both edges of the calibration range having very small magnitude (Fig. 5) which could be detrimental to the accuracy of the calibration in those frequency regions.

4. Statistical investigation of the impact of noise

The purpose of this investigation is to analyse the influence and interaction of various parameters on the success and the quality of the focused wave calibration method. Metrics to assess calibration are first established. A large number of numerical simulations of calibration are then carried out as part of a statistical analysis of the impact of noise in
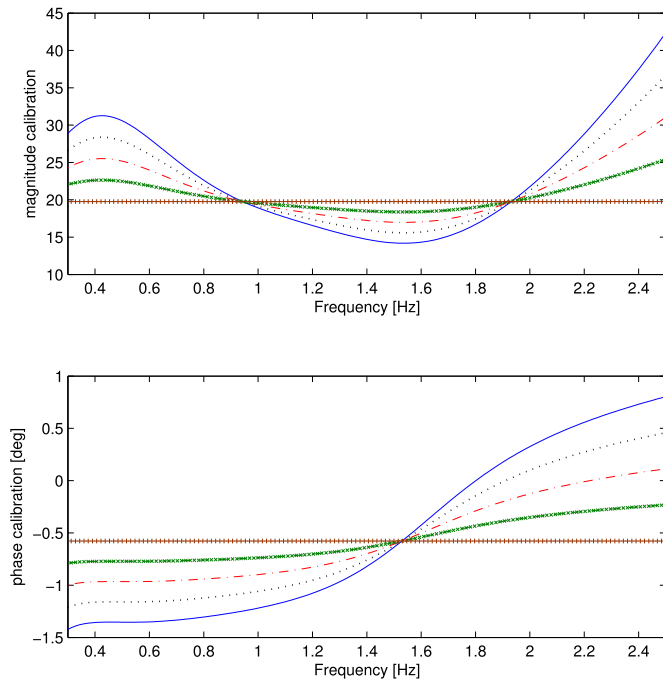
Fig. 7. The initial calibration functions used within the numerical investigation. The constant amplitude/phase calibration functions are referred to as *step 1* where the ideal calibration functions are referred to as *step 5*.

the tank transfer function on the method's performance.

4.1. Calibration metrics

4.1.1. Quality of a focused event

The goal of a focused event is to concentrate energy in a small time window. To define the quality of a focused wave event, a metric referred to as fe_{q2} and based on the ratio of significant wave height outside of the time window to the significant wave height of the complete timeseries is considered hereafter. Physically, this metric provides an indication of the square root of the ratio of the energy associated with the wave elevation timeseries outside the time window over the energy of the complete timeseries. With the calibration method only considering the energy within a specified time window, the importance of this metric is paramount. A significant amount of energy outside the window will inevitably lead to inaccurate results.

4.1.2. Quality of a random phase spectrum

The metric quantifying the quality of a generated random phase spectrum must purely assess how well the target frequency spectrum is reproduced. Any errors associated with the phase information are irrelevant in this case. The metric chosen in this context is based on the normalised discrepancy between the generated spectrum S_g and the target spectrum S_t. It is denoted as dis_{mag} and is defined as follows:

$$dis_{mag} = 100 \cdot \sqrt{\frac{1}{N} \sum_{i=1}^{N} \left(\left(\left| \frac{S_{t_i}}{S_{g_i}} \right| - 1 \right) - \mu \right)^2} \quad \text{with} \quad \mu = \frac{1}{N} \sum_{i=1}^{N} \left(\left| \frac{S_{t_i}}{S_{g_i}} \right| - 1 \right)$$

(1)

where S_{t_i} and S_{g_i} are the amplitudes of the N frequency components of spectra S_t and S_g respectively. Using $\sigma(x_i)$ to express the standard deviation of the data set $x_1, x_2, \ldots, x_N$, (1) can be written as follows:

$$dis_{mag} = 100 \cdot \sigma \left(\left| \frac{S_{t_i}}{S_{g_i}} \right| - 1 \right)$$

(2)

4.1.3. Quality of random wave time series

The ability of the tank to accurately reproduce random wave elevation time series requires both an accurate reproduction of the amplitude and the phase information. To devise a suitable metric to assess this ability, it is proposed to first compute the difference between the realised and the target wave elevation time series as:

$$\eta_{diff}(t) = \eta_{realised}(t) - \eta_{desired}(t).$$

(3)

This 'difference' time series $\eta_{diff}(t)$ is dependent on both the amplitude and the phase error in the spectrum realised in the tank. To compare the quality of different 'difference' time series, it is necessary to reduce each of them to a single number. This is achieved by estimating the *significant wave height* associated with the $\eta_{diff}(t)$ time series and then by normalising it by the significant wave height of the target spectrum. The normalised significant wave height of the 'difference' time series is noted $H_{s,diff}$ and, after simplification of the equations, it is computed as:

$$H_{s,diff} = 100 \sqrt{\frac{m_{0,diff}}{m_{0,des}}}$$

(4)

with $m_{0,diff}$ being the $zero^{th}$ moment of the $\eta_{diff}(t)$ time series, and $m_{0,des}$ being the $zero^{th}$ moment of $\eta_{desired}(t)$ time series.

4.2. Description of the numerical method

Both the effect of random noise in the tank transfer function and the departure of the initial tank calibration from the ideal calibration function are examined. Random noise can be seen as a conceptual extension of the discontinuities considered in §3.1. Further, in §3.2 it was highlighted that the combination of discontinuities and zero padding may lead to an incorrect calibration. For the purpose of the numerical investigation smooth but large differences between the initial and the ideal transfer function are introduced to evaluate the suitability of the focused event calibration method. The investigation addresses both the calibration based upon an arbitrary initial calibration function and a calibration based upon a theoretical calibration function.

First, the theoretical transfer function of a wave flume located at the University of Edinburgh was calculated, and the corresponding ideal (theoretical) calibration function was devised. To evaluate a wide range of cases, the following four modifications were introduced to the ideal calibration function:

i. Three levels of random noise in the magnitude. Each bin of the initial calibration function magnitude is modified by adding a number drown from the normal distribution and scaled by the noise level. An example of this process being illustrated in Fig. 6 (a).

ii. Three levels of random noise in the phase. Each bin of the initial calibration function phase is modified by adding a number drown from the normal distribution and scaled by the noise level. An example of this process being illustrated in Fig. 6 (b).

iii. Five levels of magnitude departures, equally spaced between the ideal calibration function and a constant amplitude calibration function; this being illustrated Fig. 7 (a).

iv. Five levels of phase departures, equally spaced between the ideal calibration function and a constant phase calibration function; this being illustrated Fig. 7 (b).

Finally, three repetitions for each of the above combinations were simulated. Considering all permutations leads to $3 \times 3 \times 5 \times 5 \times 3 = 675$ test cases. A numerical calibration routine is performed for each case, and the metrics related to focused events and time series (§4.1) are recorded. The calibration routines are terminated if convergence has not been achieved after 500 iterations. Throughout the numerical investigation, convergence is defined as a maximum magnitude departure of
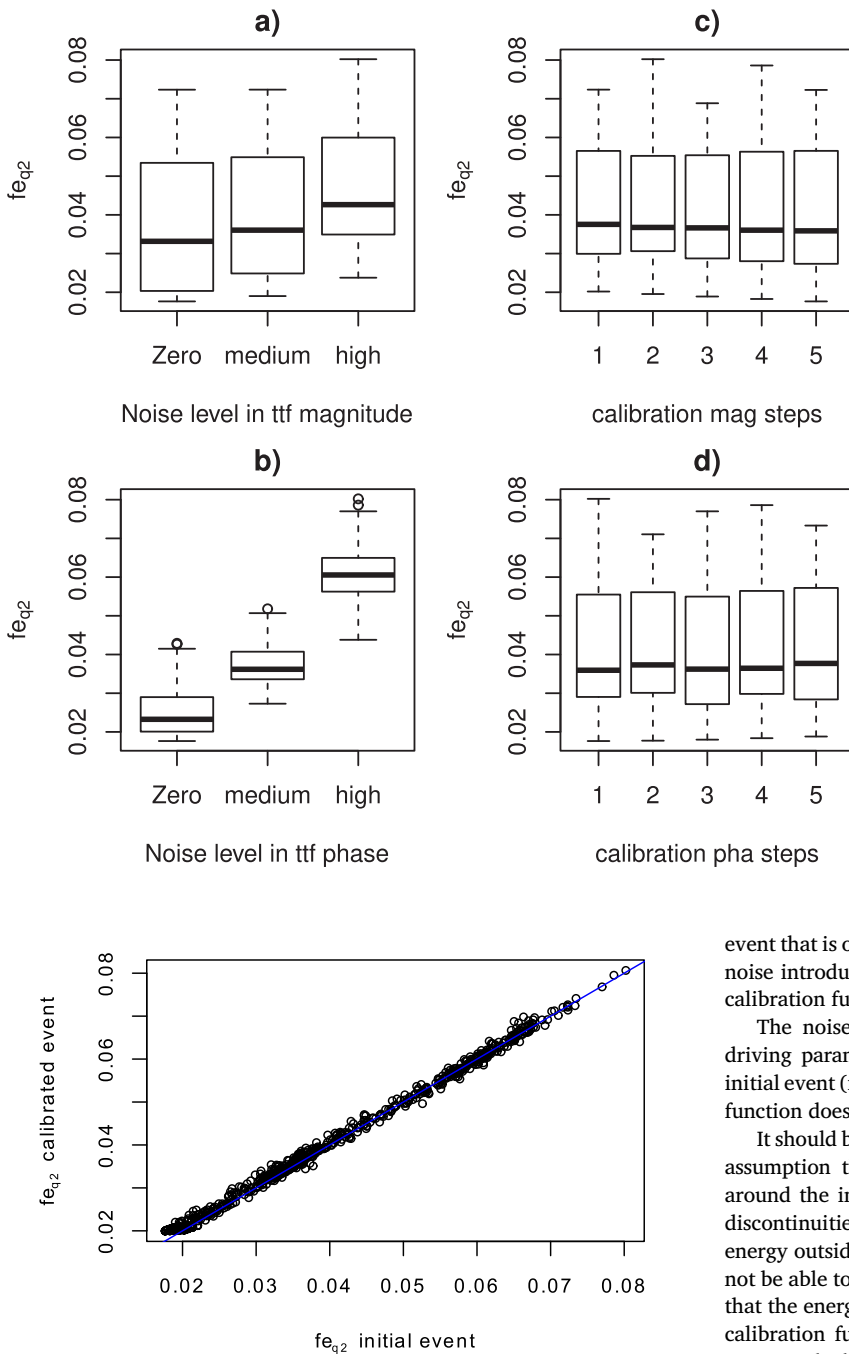
Fig. 8. Quality of the initial focused event, evaluated adopting the metric fe_{q2}, against the four types of departure introduced in the tank transfer function (ttf) and initial calibration function. The four types of departure are explained in section 4.2. Plot a) corresponds to type i, plot b) to type ii, plot c) to type iii and plot d) to type iv.

Fig. 9. Quality of the calibrated focused event against the quality of the initial focused event.

one percent and a maximum phase departure of one degree. During all tests, a JONSWAP energy distribution has been assumed; the potential advantages of different calibration spectra having already been discussed in §3.3.

The first set of simulations addresses the interdependency of (a) the tank transfer function/initial calibration function and (b) the quality of the initial focused event. Subsequently the impact of the initial focused event quality on the quality of the calibration process is examined.

4.3. Quality of the initial focused event

Using 'box-and-whisker plots' (see appendix Appendix A), Fig. 8 shows the variability of fe_{q2} for the initial focused event, which is the

event that is obtained for the uncalibrated wave tank, as a function of the noise introduced into the transfer function and the five different initial calibration functions.

The noise in the transfer function (magnitude and phase) is the driving parameter for the observed degradation of the quality of the initial event (increase of fe_{q2}). On the contrary, the initial tank calibration function does not appear to have a significant effect on it.

It should be noted once again that the calibration method relies on the assumption that the energy outside of the considered time window around the initial focused event can be ignored. The observation that discontinuities or noise in the transfer function, induce spilling of the energy outside the time window is an indication that the method might not be able to cope with such types of issues. On the other hand, the fact that the energy content outside the window is not affected by the initial calibration function shows that as far as the focused event quality is concerned, the calibration method can successfully be applied with a completely uncalibrated wave tank, provided that there is no discontinuity in the initial calibration function and in the transfer function.

4.4. Quality of the calibrated focused wave event

In §3.1, it was shown that the convergence of the method is not sufficient to ensure the quality of the final calibration function. It is possible to obtain a perfect time series in the narrow time window around the focused event with a less than satisfactory time series outside this window; this corresponding to a relatively high value of fe_{q2}. Therefore, the quality of the calibrated focused event must be assessed by considering the quantity of energy outside the narrow time window, adopting the metric fe_{q2} once again.

Fig. 9 shows the quality of the calibrated focused event as a function of the quality of the initial focused event. The calibration method appears to be unable to lead to any improvement in the fe_{q2} metric; the vast
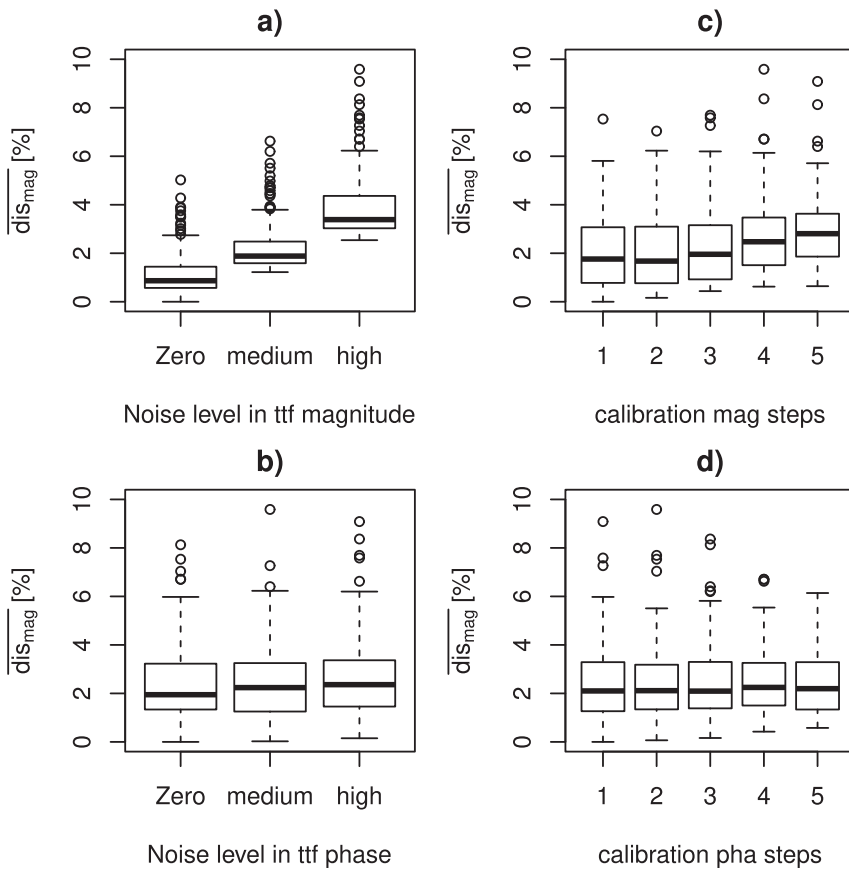
Fig. 10. Quality of calibrated random phase spectra for the four types of departure introduced in the tank transfer function (ttf) and initial calibration function. The four types of departure are explained in section 4.2. Plot a) corresponds to type i, plot b) to type ii, plot c) to type iii and plot d) to type iv. Note: A small number points lying above 10% have been ommited in the illustration.

majority of the data points lying on or close to the identity line. Consequently, in order to obtain a good focused event, it is important to start with a good initial focused event as measured by fe_{q2}. According to Fig. 8, the quantity of energy outside the measurement window for the initial event is predominately related to the noise introduced in the transfer function; the magnitude and phase of the initial transfer function only affecting this measure marginally.

4.5. Quality of a random phase spectrum after calibration

One of the main objectives of tank calibrations is to improve the quality of wave spectra generated in the tank. The quality of the generated spectra mainly depends on the quality of the magnitude calibration. However, errors in the phase calibration may also have a slight influence on the magnitude calibration. The fidelity of the produced power spectra must consequently be investigated with respect to the four sources of departures considered above.

The mean of the discrepancy dis_{mag} between a target JONSWAP spectrum and the calibrated spectrum is plotted against the four considered parameters and shown in Fig. 10. As expected, the phase calibration does not have any significant influence on the quality of the power spectra. The level of noise in the magnitude of the transfer function appears to be the most important parameter. This confirms that the calibration method struggles to handle sharp discontinuities in the transfer function or the initial calibration function. On the other hand, in the absence of such discontinuities and with an erroneous but smooth initial calibration function, the calibration method yields good results in terms of generated power spectra.

4.6. Quality of random wave time series after calibration

The last objective of the tank calibration process is to improve the

ability of the tank to generate random wave time series at one point in the tank. How well the generated wave time series matches its target is affected both by the magnitude calibration and the phase calibration.

The $H_{s,diff}$ of a calibrated time series based on a JONSWAP spectrum is investigated against the four considered parameters as shown in Fig. 11. Concerning the quality of the calibrated focused event, the level of noise in the phase transfer function appears to be the most important source of error in the calibrated time series (Fig. 11 a). The level of noise in the magnitude transfer function is also important as seen in Fig. 11 c, whereas the initial calibration function of the tank appears irrelevant (Fig. 11 b and d). This is a further confirmation that the calibration method struggles to handle sharp discontinuities in the transfer function or the initial calibration function.

5. Conclusions and recommendations for tank calibrations

The present paper has numerically investigated the range of applicability of the focused wave calibration method developed by Masterton and Swan (2008) for forced controlled wave makers beyond its original intended use for focused waves applications. In doing so, a potential pitfall of the original method has been highlighted. Problems can indeed occur if the transfer function of the wave tank or if the initial calibration function used are discontinuous. In this case, the calibration method can be deceptive in that it converges towards what appears to be a suitable calibration function. In fact, after such erroneous calibration, generated waves match the target sea only within the bounds of the measurement time window. The paper has demonstrated that the limitation of the method is due to the zero padding process.

The performance of the method has been quantitatively assessed for the generation of focused events, random phase spectra and random wave time series. This assessment relies on a statistical approach and has led to the development of new metrics. Results show that for focused
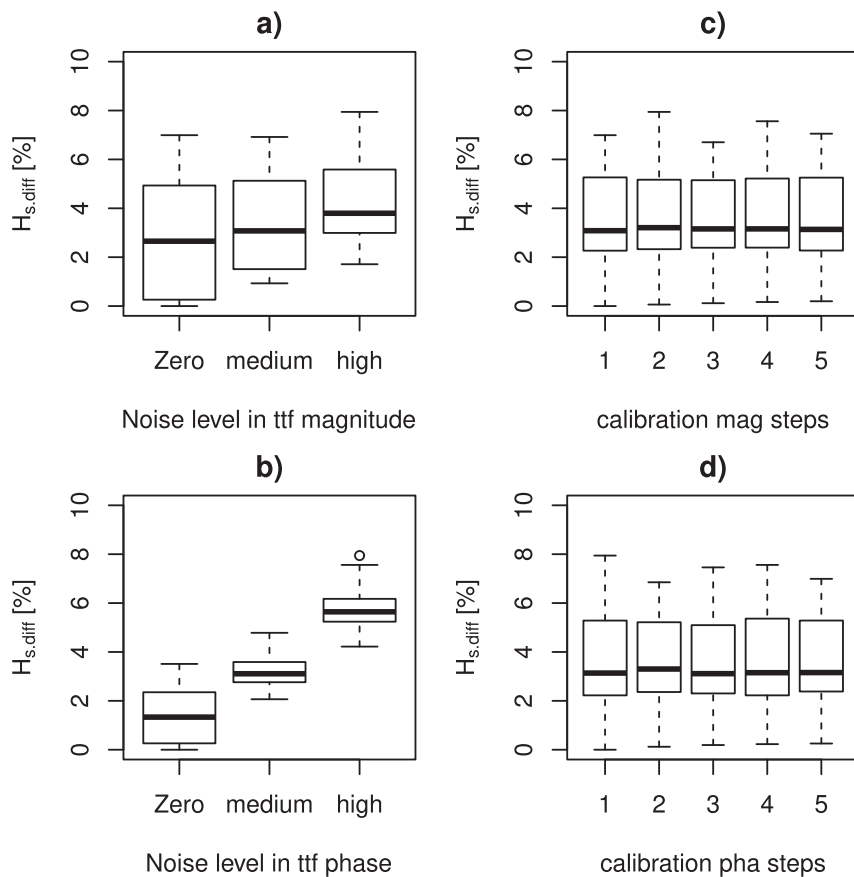
Fig. 11. Quality of the calibrated time series for the four types of departure introduced in the tank transfer function (ttf) and initial calibration function. The four types of departure are explained in section 4.2. Plot a) corresponds to type i, plot b) to type ii, plot c) to type iii and plot d) to type iv.

wave generation and random wave time series, the method is affected by noise both in magnitude and phase of the initial calibration function. Random phase spectra generation is predominantly affected by noise in the magnitude. The actual value of the initial calibration function, provided that it is smooth, has very little impact on the method performance for any type of sea states.

The paper has also explored alternative spectra to the JONSWAP spectrum used by Masterton and Swan (2008). The simulations show that Hamming and Hanning spectra can focus more energy within a very limited time window than a JONSWAP spectrum.

In light of the above, the method of Masterton and Swan (2008) is very useful and efficient for general wave tank calibration provided that a number of precautions are taken. It should be made sure that the initial calibration function used is smooth. Ideally, one should use the inverse of the theoretical transfer function. If it is not available, it is better to use a completely erroneous initial calibration function provided that it is smooth rather than a partially good but discontinuous one. This could happen when the initial calibration function used is a 'composite' made of the usually smooth calibration function supplied originally with the facility and of a frequency sub-range which has been later on calibrated experimentally using regular waves. This composite calibration function could exhibit discontinuities at the edges of the experimentally calibrated frequency sub-range where it transitions to the original calibration function. The method should not be used if the transfer function of the tank is likely to include discontinuities. This could happen for example with wet back wave makers where the sloshing occurring at the back of the paddle could induce such discontinuities. Finally, the original method could be improved by relying on Hamming or Hanning spectrum rather than a JONSWAP one.

Linear wave theory was applied throughout this paper. In large wave group or steep sea state generation, nonlinear wave-wave interactions are clearly of concern. Unfortunately, there is no effective methodology to

date that combines the benefits of an empirical calibrations discussed here with nonlinear approaches such as second-order wavemaker theory. This remains a challenging area of research, and is suggested for future research.

Acknowledgments

Appendix A. Box and whisker plot

The box plots shown in Figs. 8, 10 and 11 are used to represent the effect of categorical explanatory variables (factors) with two or more levels. The horizontal bold line of a box plot (sometimes also referred as 'box-and-whisker plot') shows the median of the observations. The bottom and top of the box are located at the first and third quartiles. As a result, effectively 50% of the data are contained *inside* the box. The dashed lines outside of the box, the 'whiskers', extend to the minimum and the maximum of the data or to 1.5 times the interquartile range (roughly 2 standard deviations) if the latter is smaller. In the latter case, observations falling outside the 'whiskers' are called outliers. Box plots, in effect, give good visual information about the data, its location and skewness. Outliers can be a sign of errors and should normally be investigated. Comparing box plots from different levels of a factor gives information about the significance of the difference of mean between the levels. Principally, if the median value of one level lies outside the box of another level, this provides a good indication that the difference of mean is significant, i.e. that the parameter has a significant effect to explain the observed variability of the data.

References

Biésel, F., Suquet, F., 1954. Laboratory Wave Generating Apparatus. St. Anthony Falls Hydraulic Laboratory,University of Minnesota,Minneapolis. Project Report No. 39.

Havelock, T.H., 1929. Forced surface-wave on water. Phil. Mag. viii, 569–576.

Latheef, M., Swan, C., 2013. A laboratory study of wave crest statistics and the role of directional spreading A laboratory study of wave crest statistics and the role of directional spreading. Proc. Roy. Soc. 469 (February), 1–24.

Masterton, S., Swan, C., 2008. On the accurate and efficient calibration of a 3d wave basin. Ocean Eng. 35 (8–9), 763–773.

Reich, A., 2010. Calibration of a Unidirectional Wave Flume Using a Transient Focused-wave Approach. Master's thesis. The University of Edinburgh.

Spinneken, J., Swan, C., 2009a. Second-order wave maker theory using force-feedback control. Part I: a new theory for regular wave generation. Ocean Eng. 36 (8), 539–548.

Spinneken, J., Swan, C., 2009b. Second-order wave maker theory using force-feedback control. Part II: an experimental verification of regular wave generation. Ocean Eng. 36 (8), 549–555.

Spinneken, J., Swan, C., 2011. Theoretical transfer function of force-controlled wave machines. Int. J. Offshore Polar Eng. 21, 169–177.

Spinneken, J., Swan, C., 2012. The operation of a 3d wave basin in force control. Ocean Eng. 55, 88–100.

Ursell, F., Dean, R., Yu, Y., 1960. Forced small-amplitude water waves: a comparison of theory and experiment. J. Fluid Mech. 7, 33–52.